

Transient Porosity Resulting from Fluid–Mineral Interaction and its Consequences

Andrew Putnis

*The Institute for Geoscience Research (TIGeR)
Curtin University, Perth, Australia*

and

*Institut für Mineralogie, University of Münster
Münster, Germany*

putnis@uni-muenster.de; andrew.putnis@curtin.edu.au

INTRODUCTION

The term *porosity* is very widely used in geosciences and normally refers to the spaces between the mineral grains or organic material in a rock, measured as a fraction of the total volume. These spaces may be filled with gas or fluids, and so the most common context for a discussion of porosity is in hydrogeology and petroleum geology of sedimentary rocks. While porosity is a measure of the ability of a rock to include a fluid phase, *permeability* is a measure of the ability for fluids to flow through the rock, and so depends on the extent to which the pore spaces are interconnected, the distribution of pores and pore neck size, as well as on the pressure driving the flow.

This chapter will be primarily concerned with how reactive fluids can move through ‘tight rocks’ which have a very low intrinsic permeability and how secondary porosity is generated by fluid–mineral reactions. A few words about the meaning of the title will help to explain the scope of the chapter:

(i) “Fluid–mineral interaction”: When a mineral is out of equilibrium with a fluid, it will tend to dissolve until the fluid is saturated with respect to the solid mineral. We will consider fluids to be aqueous solutions, although many of the principles described here also apply to melts. The generation of porosity by simply dissolving some minerals in a rock is one obvious way to enhance fluid flow. Dissolution of carbonates by low pH solutions to produce vugs and even caves would be one example. However, when considering the role of fluid–mineral reaction during metamorphism the fluid provides mechanisms that enable re-equilibration of the rock, i.e., by replacing one assemblage of minerals by a more stable assemblage. This not only involves the dissolution of the parent mineral phases, but the reprecipitation of more stable product phases while the rock remains essentially solid through the whole process, even though the reactions require permeability for fluid transport. This latter aspect of fluid–mineral interaction will be one focus of this chapter.

The interpretation of mechanisms of reactions in rocks is based on studying the microstructural development associated with the reaction. The microstructure of a rock describes the relationships between the mineral grains and organic material in the rock, their size, shape, and orientation. When reactions involve fluids we look for microstructural and chemical evidence for the presence of fluid and fluid pathways. In that sense the porosity can be considered as an integral part of the microstructure, in that it is the space occupied by the fluid phase, and the distribution of the fluid phase is just as important to the rock properties as the distribution of the minerals.

The individual mineral grains in a rock may also have a microstructure that reflects the processes taking place within the crystalline structure as a result of the geological history of the rock. Examples would include exsolution from an initial solid solution, or transformation twinning, or the formation of dislocation arrays during deformation. The rock and mineral microstructures can provide important information on how the rock formed and its subsequent thermal and deformational history. The microstructure is thus a direct result of the mechanisms of the processes that take place when a rock or mineral reacts to lower the overall free energy of the system under the imposed physical and chemical conditions. The microstructure formed during any process is always a balance between the thermodynamics (reducing the free energy) and the kinetics (the time available and the rates of the processes involved). As such, a microstructure may change over time, for example by coarsening or recrystallization to reduce the surface energy.

(ii) “Transient porosity”: If we consider that the porosity is that part of the microstructure occupied by the fluid phase, then it is also subject to re-equilibration over a period of time. Just as porosity in poorly consolidated sediments is modified during diagenesis, compaction and pressure solution, porosity generated by fluid–mineral reactions will also be modified with time. The rate of fluid–mineral reactions is orders of magnitude faster than solid state reactions in which mass transfer takes place by slow diffusional processes (Dohmen and Milke 2010; Milke et al. 2013) and so some porosity microstructures generated by fluid–mineral reactions may be considerably “more transient” than microstructures generated by solid state mechanisms, e.g., exsolution. The “closure temperature” at which a specific microstructure or chemical distribution is frozen in time and available for study is much higher when the re-equilibration mechanism depends on solid state diffusion than if reactant or product transport through fluids is involved.

(iii) The “Consequences” discussed in this chapter will be mainly concerned with the supersaturation of fluids in pores and hence the role of porosity in controlling nucleation and growth of secondary minerals in the pore spaces.

FLUID–MINERAL INTERACTIONS: PRESSURE SOLUTION

When an aqueous fluid interacts with a mineral with which it is not in equilibrium (i.e., is either undersaturated or supersaturated with respect to that mineral) the mineral will either tend to dissolve or grow until equilibrium is reached, i.e., until the fluid is saturated with respect to that mineral. The solubility of a mineral can also be increased by applied stress and this leads to the phenomenon of pressure solution whereby grains in contact with one another and under compression dissolve at these pressure points. The resulting fluid is then supersaturated with respect to a free mineral surface and can reprecipitate in the pore spaces (Fig. 1). The newly precipitated phase may have the same major chemical composition as the dissolved phase, but can be recognized as an overgrowth both texturally and from trace element and isotope geochemistry (Rutter 1983; Gratier et al. 2013). This mechanism of compaction reduces the porosity of a rock and leads to well-known relationships between depth of burial, porosity and rock density (e.g., Bjørlykke 2014 and refs therein). The reprecipitated phase can also act as a cement to bind the particles during the lithification process.

Pressure solution is usually invoked to describe compaction during burial of mineralogically simple sedimentary rocks (such as sandstone and limestone) at relatively low temperatures. Theoretical models of pressure solution usually assume mono-mineralic rocks. Even when two minerals with different dissolution rates or hardnesses are in contact, chemical reactions between them and the solution are usually not considered, although the enhancement of the pressure solution of quartz by the presence of clays has been recognized for many years (Renard et al. 2007). The effects of pressure solution on rock microstructure can be

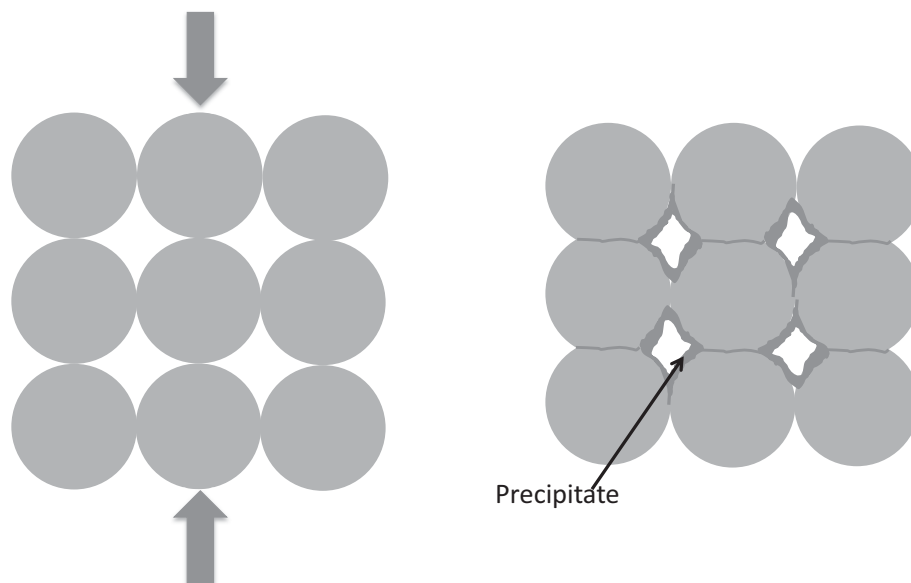


Figure 1. Schematic drawing of pressure solution. A material under applied stress dissolves at the stress points, where the spherical grains are in contact, and is transported through the solution to sites of lower stress where it reprecipitates. Compaction by pressure solution reduces the porosity and permeability of a rock.

readily identified, as can the reduction in pore space. Such effects are principally of concern to evaluating fluid flow in sedimentary rocks and have been summarized in many books and review papers (e.g., Jamtveit and Yardley 1997; Parnell 1998).

However, the general principles in pressure solution, i.e., dissolution–transport–precipitation, also apply to deeper crustal rocks, where the transport of material by pressure solution creep can result in large scale rock deformation (Gratier et al. 2013).

FLUID–MINERAL INTERACTIONS: MINERAL REPLACEMENT

A more general scenario than that applied to simple pressure solution is the situation that when a mineral or rock reacts with a fluid with which it is out of equilibrium, it will start to dissolve and result in a new fluid composition at the fluid–mineral interface which is supersaturated with respect to some other mineral phase, or phases. Thus the dissolution of the parent phase may result in the precipitation of a new, more stable phase. From basic thermodynamic considerations, the more stable phase will be less soluble in the specific fluid composition than the parent dissolving phase.

The spatial relationships between the dissolution and precipitation will depend on the rate-controlling step in the sequence of processes of dissolution–transport–precipitation. If dissolution and transport are fast relative to precipitation then the components in the supersaturated fluid may migrate some distance through a rock before precipitation takes place, and the parent and product phases may be spatially separated. This would be the case if overall the system was rate limited by precipitation. However, from a study of natural rock textures as well as experimental reactions, a more common situation is that dissolution is the rate-controlling step and that precipitation is fast relative to dissolution (Wood and Walther 1983; Walther and Wood 1984; Putnis 2009). In such a case precipitation is closely coupled to the dissolution, and may actually take place on the surface of the dissolving parent phase.

Close spatial and temporal coupling of dissolution and precipitation leads to pseudomorphic mineral replacement in which the product phase has the same external dimensions and shape as the parent. The mechanism of such *interface-coupled dissolution–precipitation* has been described in a number of review papers (Putnis 2009; Ruiz-Agudo et al. 2014) and so only the briefest account will be given here. In the rest of this chapter the term “parent phase” refers to the mineral which is dissolving in the fluid, and the “product phase” is the reprecipitated phase from the resultant solution. The important point to note is that porosity generation in the product phase is a necessary prerequisite for pseudomorphic replacement to take place.

The general principles can be illustrated with the aid of a schematic diagram (Fig. 2). The dissolution of even a few monolayers of the parent mineral may result in a localized supersaturation at the fluid–mineral interface relative to a new phase. This phase could then nucleate on the dissolving mineral surface (Fig. 2a,b). Nucleation would be enhanced if there is some crystallographic matching (epitaxy) between the parent and the product phase (e.g., one feldspar replaced by another, Niedermeier et al. (2009); Norberg et al. (2011)). However the lack of epitaxial relations between parent and product phases does not preclude pseudomorphic replacement as shown by the replacement of calcite by apatite, which have no obvious structural features in common (Kasioptas et al. 2011). In the former case where there is good crystallographic matching across the parent product interface, a single crystal of the parent can be replaced by a single crystal of the product. In the latter case the product phase is polycrystalline. The coupling between the dissolution and precipitation ensures that the new phase preserves the external shape of the parent.

The next step in the process is crucial. Unless there are transport pathways maintained between the external fluid reservoir and the interface between the parent and the product phases, an impermeable layer of the new phase could isolate the parent from the fluid and the reaction would stop with equilibrium only established between the new rim and the fluid. Thus for the reaction to proceed instead of armoring the reacting crystal (e.g., Velbel 1993), the new phase must have interconnected porosity (Fig. 2c).

The generation of porosity depends on two factors: (i) the molar volume difference between the parent and product phases, and (ii) the relative solubility of the parent and product phases in the specific reactive fluid.

If the molar volume associated with a replacement process increases, as is the case of aragonite being replaced by calcite (Perdikouri et al. 2011) this will tend to militate against porosity generation. If under the conditions of any experiment or natural system calcite is

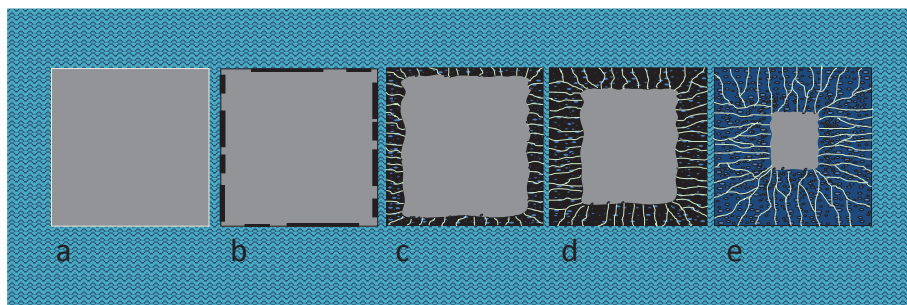


Figure 2. Schematic drawing of a pseudomorphic replacement reaction. When a solid (a) is out of equilibrium with an aqueous solution, it will begin to dissolve. The resulting fluid composition at the interface with the solid may become supersaturated with respect to another phase and (b) precipitate on the surface of the dissolving solid. This sets up a feedback between dissolution and precipitation. For the dissolution–precipitation reaction to continue (c–e), the precipitated phase must have interconnected porosity, allowing fluid access to the reaction interface and diffusion of components through the fluid

more stable than aragonite, then calcite will be less soluble than aragonite. This means that more of the aragonite will be dissolved than calcite precipitated and some Ca^{2+} and CO_3^{2-} ions will go into the solution. This second factor will tend to outweigh the first, as for any reaction to proceed, the thermodynamics will dictate that the product must be less soluble, in the specific solution from which it precipitates, than the parent. If interconnected porosity is generated then the reaction will proceed and result in a porous, and hence turbid, pseudomorph of the original phase (Fig. 2d,e). Turbidity or cloudiness in a crystal is usually associated with porosity or the presence of many fine inclusions and can be the first indication that a mineral is the result of a secondary replacement.

The model salt system in which such a mechanism has most thoroughly been examined is $\text{KBr-KCl-H}_2\text{O}$ (Putnis and Mezger 2004; Putnis et al. 2005; Pollok et al. 2011; Raufaste et al. 2011). In particular, Pollok et al. (2011) have analyzed the progressive replacement of one salt by another, taking into account the solid:fluid ratio, the changing chemistry of the fluid, and the evolution of the chemistry of the solid. As there is complete solid solution between KBr and KCl , the replacement proceeds progressively in composition, by continuously re-equilibrating the solid composition as the fluid composition evolves (Putnis and Mezger 2004). In this system the porosity has also been shown to evolve with time while the replaced and porous crystal remains in contact with the fluid with which it has chemically equilibrated (Putnis et al. 2005; Raufaste et al. 2011). Thus textural equilibration, also by dissolution and reprecipitation, follows chemical equilibration and porosity may ultimately be completely removed. The dynamic nature of porosity and its eventual annihilation by coarsening has also been observed in experiments on feldspar replacement by Norberg et al. (2011).

Although in the examples above the porosity is a dynamic and transient feature of fluid–mineral interaction, it is possible that a fluid-filled pore may also be stable especially on grain boundaries, depending on the balance of surface tensions between two solid surfaces and the solid–fluid interfaces (von Bargen and Waff 1986; Watson and Brennan 1987; LaPorte and Watson 1991; Lee et al. 1991).

POROSITY AND FELDSPAR–FELDSPAR REPLACEMENT

The presence of turbidity and related porosity in feldspars from many different geological environments has been noted in the literature for many years. After the initial studies which demonstrated that turbidity in feldspars was due to porosity and the association with crystallization in a fluid-rich environment (Folk 1955; Montgomery and Brace 1975), detailed petrography in alkali feldspars (Parsons 1978; Walker 1990; Worden et al. 1990; Guthrie and Veblen 1991; Waldron et al. 1993; Walker et al. 1995; Parsons and Lee 2009) demonstrated that porosity was often associated with fluid-induced sub-solidus alteration and coarsening, e.g., cryptoperthite coarsening to patch perthite, as well as orthoclase coarsening to microcline. More recently it has been demonstrated experimentally that the development of patch perthite from cryptoperthite involves porosity generation (Norberg et al. 2013).

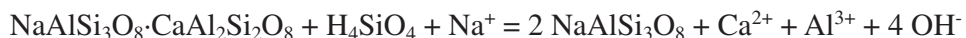
In the examples above the replacement of one feldspar by another was essentially isochemical and driven by the reduction in strain energy. Strained feldspar (as is the case with the coherently exsolved alkali feldspars and the coherent transformation twinning in orthoclase) is more soluble than patch perthite and microcline in which the internal interfaces are incoherent, and hence the generation of porosity is a result of this difference in solubility rather than any molar volume effects.

Porosity is also generated when a feldspar is replaced by another with different composition. The most common example is albitization which generally refers to the replacement of any feldspar by almost pure albite. It is one of the most common aluminosilicate reactions in

the shallow crust of the earth (Perez and Boles 2005) and takes place whenever feldspar is in contact with saline aqueous solutions. Albitization is common during the diagenesis of arkosic sediments as well as taking place at higher hydrothermal temperatures. The porosity associated with the pseudomorphic albitization of natural plagioclase has been noted by many authors (e.g., Boles 1982; Lee and Parsons 1997; Lee and Lee 1998; Engvik et al. 2008).

For example, albitization is widespread in the crystalline rocks of the Bamble Sector, south Norway where the replacement of plagioclase by albite is also associated with reddening of the rock. Figure 3a is a BSE SEM image of a polished cross-section of a specimen from a Norwegian outcrop showing a partially replaced plagioclase grain. On the right of this figure the plagioclase phase is oligoclase and on the left the darker contrast phase is albite. The black spots are pores which have remained unchanged since the albitization event over a billion years ago (Nijland et al. 2014). The largest pores are up to several microns and the smallest are below the resolution of the image. TEM observations of the same sample (Engvik et al. 2008) show that the pore size varies down to a few nanometers. The pale laths in Figure 3a are hematite, which is associated with the albitization and causes reddening.

The pseudomorphic albitization reaction for an intermediate plagioclase (Merino 1975; Perez and Boles 2005) could be represented by:



where the silica required for the reaction is in solution together with the Na^+ ions. The equation makes the approximation that intermediate plagioclase has the same molar volume as albite. To account for the porosity some of the silicate must also stay in solution, and this is not taken into account in the equation above. This requires that both Ca and Al are released into solution.

Note: A pseudomorphic replacement reaction implies preservation of the external volume and shape of the original parent crystal (i.e., the total volume of the product phase plus generated pore volume equals the volume of the parent crystal.). The albitization equation above is written to preserve volume and this inevitably implies mobility of Al. However whether a reaction is pseudomorphic or not depends entirely on the composition and pH of the fluid phase. In determining mass balance during mineral replacement (e.g., using Gresens' analysis) an assumption has to be made as to whether the volume is preserved, as above, or whether a specific element (typically Al) is immobile. This problem discussed in detail in Putnis (2009) and in Putnis and Austrheim (2012).

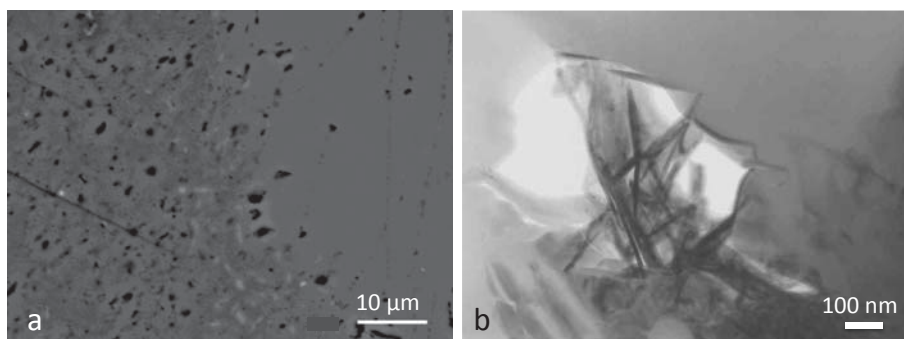


Figure 3. (a) A back-scatter electron (BSE) image of an albitization reaction front in a plagioclase single crystal from partly albitized rock in the Bamble Sector, south Norway. The smooth textured phase on the right is the parent oligoclase and the darker phase on the left is the product albite. The black spots in the albite are pores. The lighter laths are sericite. (b) During replacement of feldspars hematite may crystallize within the pore-spaces, giving the rock a reddish color, such as commonly seen in pink granites.

Although the pseudomorphic replacement of plagioclase by albite generates porosity and hence may increase the permeability of a rock, complications arise if the ions released to solution also precipitate another phase. For example, the release of Al creates the possibility of reaction with excess silica in solution to form kaolinite, which would reduce the permeability.

In experiments on the albitization of plagioclase, Hövelmann et al. (2010) found that needles of pectolite ($\text{NaCa}_2\text{Si}_3\text{O}_8\text{OH}$) formed within the pores generated within the albite. These experiments were carried out at 600 °C and 2 kbars, and at those temperatures reaction rims up to 50 μm wide formed within 14 days. Norberg et al. (2011) studied the microstructural evolution during experimental albitization of K-rich alkali feldspar, a reaction that only involved the ion-exchange of K by Na. They found that the ion-exchange mechanism was not a simple diffusional exchange, but involved interface-coupled dissolution–precipitation and the generation of porosity. Furthermore they made the important observation that the porosity and connectivity of the pores is dynamic and continuously evolves during the replacement process. A similar observation was made by Putnis and Mezger (2004) and Raufaste et al. (2011) for the replacement of KBr by KCl.

Albitization is a ubiquitous process in the Earth's crust because of the wide availability of Na-rich saline aqueous solutions. However it is also common to find plagioclase replaced by K-feldspar, again with the generation of porosity (e.g., Schermerhorn 1956; Harlov et al. 1998; Putnis et al. 2007).

The replacement of one feldspar by another in nature, whether it be plagioclase replaced by K-feldspar or by albite, is frequently associated with the precipitation of hematite, which gives these feldspars a pink color. A study of pink feldspars in granites from a number of localities (Putnis et al. 2007; Plümper and Putnis 2009) has shown that the hematite forms nano-rosettes within the pore spaces generated during the feldspar replacement (Fig. 3b). The conclusion from these studies was that pink feldspars indicated that the original rock has been infiltrated by an Fe-bearing solution and that the feldspar replacement also initiated hematite precipitation, possibly due to a local change in pH at the reaction interface.

In general, the presence of porosity and hence turbidity in natural feldspars is characteristic of replaced feldspars (Parsons 1978; Worden et al. 1990) although the absence of porosity does not necessarily indicate that the phase is primary. Dalby et al. (2010) report on albite whose trace element composition indicates that it is a product of secondary albitization, i.e., the replacement of a pre-existing feldspar by albite. However, the albite is not turbid and they suggest that this could be due to textural equilibration. Martin and Bowden (1981) have also reported non-turbid secondary albite in granite. As noted above, porosity generation and its interconnectivity has been shown in experimental systems to be a dynamically evolving process.

SECONDARY POROSITY ASSOCIATED WITH MINERAL REPLACEMENT—A UNIVERSAL PHENOMENON

Although the section above has emphasized porosity generation during interface-coupled dissolution–precipitation in feldspars, Putnis and Putnis (2007) and Putnis (2009) have argued that mineral replacement by this mechanism is the universal mechanism of re-equilibration of solids in the presence of a fluid phase and that porosity generation is an integral part of this mechanism. Many examples of other systems have been described in previously published reviews and will not be given again here (see Putnis 2002, 2009; Putnis and Austrheim 2010, 2012; Putnis and John 2010; and Ruiz Agudo et al. 2014).

The porosity generated may take a number of forms. In the examples described above, the porosity appears as apparently unconnected pore space at the spatial scale of the observation

(e.g., Fig. 3b). However, during the replacement process there must be connectivity between the fluid reservoir and the reaction front suggesting that the porosity and permeability is a dynamically evolving feature (Norberg et al. 2011; Raufaste et al. 2011). However, when there is a large volume difference between the parent and product, the porosity takes on a form which resembles fluid-induced fracturing (Røyne et al. 2008; Jamtveit et al. 2009; Navarre-Sitchler et al. 2015, this volume; Røyne and Jamtveit 2015, this volume). Fluid-induced fracturing is usually associated with replacement involving a positive volume change, such as in hydration reactions during weathering (Fletcher et al. 2006; Buss et al. 2008) and the serpentinization of olivine (Iyer et al. 2008). However, Janssen et al. (2010) found that during the reaction of ilmenite (FeTiO_3) with acid to form rutile (TiO_2), a pseudomorphic replacement which involves a 40% reduction in solid volume, the reaction interface moves through the crystal by the generation of microfractures (Fig. 4). Rutile nucleates as nanoparticles from the solution formed in the microfractures. At present there is no clear understanding of the factors that control the morphology of the porosity.

IMPLICATIONS OF MICROPOROSITY— SUPERSATURATION AND CRYSTAL GROWTH

Fluid–mineral interaction is a ubiquitous process throughout the geological history of a rock, from its first formation through to weathering and destruction. The porosity and its

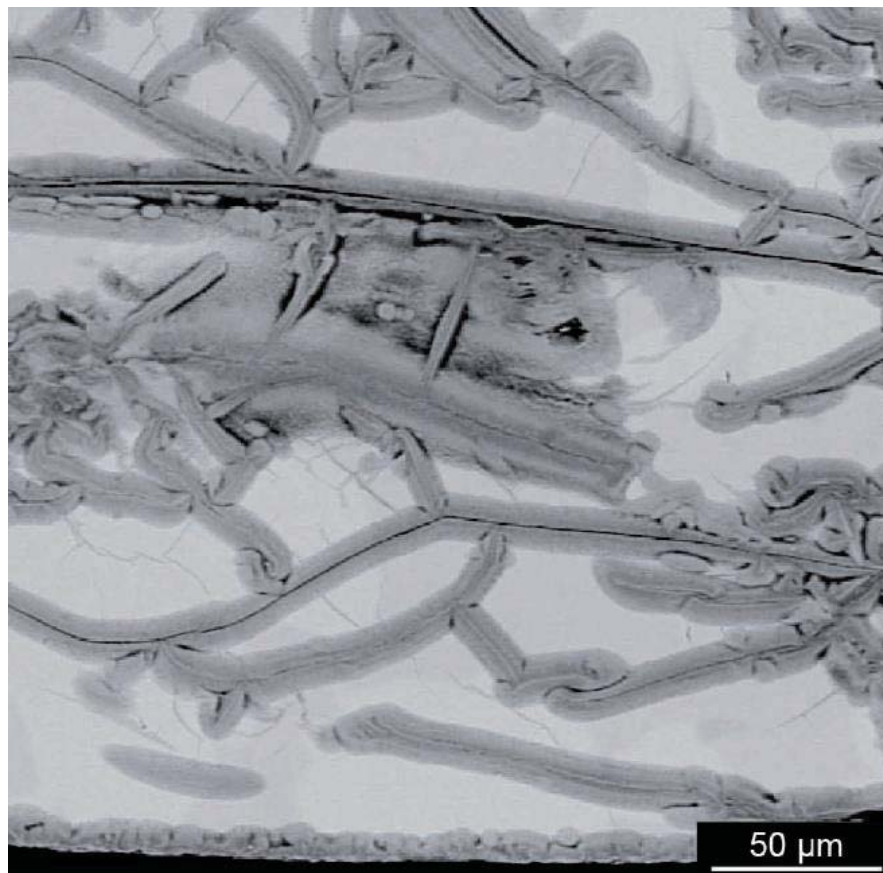


Figure 4. A back-scatter electron (BSE) image of a cross-section through an ilmenite crystal (FeTiO_3) partly replaced by an Fe-poor phase, which eventually results in the whole crystal being replaced by rutile. The “leaching” of the Fe from the ilmenite takes place by the generation and propagation of fractures (dark) through the unaltered ilmenite and precipitation of rutile from the fluid in the fractures. (See Janssen et al. 2010).

distribution play a major role in controlling the processes involved at every stage. The reaction products of fluid–mineral interaction nucleate from the fluid phase, and the free energy drive for precipitation can be expressed in terms of the supersaturation of the fluid with respect to the precipitating phase or phases. In the rest of this chapter we will review the concept of supersaturation, the degree of supersaturation required to nucleate a new phase, and how these concepts need to be modified when discussing nucleation in a porous rock.

Because crystallization in porous rocks has such wide fields of interest and many diverse applications, it has been discussed for many years from different viewpoints. The porosity and permeability of a reservoir rock is a key parameter which determines the efficiency of fluid flow, whether this be oil, gas, or hot water, and therefore precipitation within the pore space and hence permeability reduction is a major concern (Jamtveit and Yardley 1997). In a different field, salt crystallization in porous stonework and concrete is known to cause sufficient damage to break up the stone due to the “force of crystallization” associated with growing crystals pushing on pore walls (Rodriguez-Navarro and Doehne 1999a; Scherer 1999; Espinoza-Marzal and Scherer 2010). The force of crystallization is related to the supersaturation (Steiger 2005a,b). The mechanism of frost heaving is another closely related area of research where undercooled (i.e., supersaturated) water within the pore spaces in fine-grained silt migrates to the surface and crystallizes forming an ice hill (a pingo) whose weight is supported by the force of crystallization of the ice below (Ozawa 1997).

In all of these studies the fundamental premise is that a high fluid supersaturation (or undercooling in the case of ice crystallization) can be maintained in finely porous materials relative to the supersaturation at which nucleation takes place in an open system. Furthermore, the finer the porosity the higher the supersaturation in the fluid that can be maintained before crystallization can take place. To understand why this may be the case we will first examine the various concepts used to describe supersaturation and its relationship to nucleation.

Critical and threshold supersaturation

Supersaturation in an open system is defined as the ratio between the activity product in solution and the solubility constant of the mineral. For a sparingly soluble salt such as barite, the degree of saturation is defined as Ω :

$$\Omega = \{Ba^{2+}\} \cdot \{SO_4^{2-}\} / K_{sp}. \quad (1)$$

For nucleation to take place a certain *critical supersaturation* where $\Omega > 1$ must be reached to provide a driving free energy. This is usually derived from classical nucleation theory (CNT), which is simply based on thermodynamic arguments of balancing the increase in surface energy in forming a nucleus with the decrease in free energy associated with the nucleation (Fig. 5a). As the supersaturation increases, the value of the activation energy for nucleation decreases and at some critical value of the supersaturation the nucleation rate very rapidly increases (Fig. 5b). This value is taken as the critical supersaturation. Although CNT has obvious shortcomings, such as the definition of a surface energy when applied to a sub-critical nucleus, equations derived from this theory have been applied to experimental nucleation data for decades. From CNT (Nielsen 1964) the general form of the equation which describes the rate of heterogeneous nucleation in a solution, J , (i.e., the number of nuclei formed in a fixed volume) is:

$$J = \Gamma \exp\left(\frac{-\delta\sigma^3 Y^2}{k^3 T^3 (\ln S)^2}\right), \quad (2)$$

where δ is a shape related factor, σ is the fluid–mineral interfacial energy of the nucleus, Y is the volume of a growth unit in the nucleus, k is Boltzmann’s constant, T is temperature and

S is the supersaturation (in this case more simply defined as the ratio of concentration in the solution to the concentration at equilibrium). The pre-exponential factor Γ is related to the rate at which the nucleus can grow to a supercritical size, and hence it involves diffusion of growth units to the surface of the nucleus.

This equation shows that the value of the nucleation rate is a very sharp function of the supersaturation (Fig. 5b) and also that salts with a large surface energy (σ) (and hence low solubility) and large molar volume (Y) require a higher value of supersaturation for nucleation to become measurable. The shape of the nucleation rate function (Fig. 5b) leads to the general concept of a *critical supersaturation*, at which nucleation becomes spontaneous. This equation is based on the assumption that the supersaturation is a fixed value, reached instantaneously and takes no account of how the supersaturation is reached, in other words it does not take into account gradients in supersaturation either in space or in time.

However, the actual value of the supersaturation that is achieved in any given system depends on the rate of change of supersaturation. This is a well-known phenomenon in cooling melts for example: the cooling rate will determine the degree of undercooling at which crystallization takes place. In an aqueous solution, supersaturation gradients will also exist due to cooling and evaporation rates as well as due to the diffusion-controlled compositional gradients in space around a nucleus. In any real system, supersaturation gradients are unavoidable and so must be included in any treatment of nucleation from solution. The actual value of the supersaturation at which nucleation becomes measurable, as a function of supersaturation gradients, however achieved, is termed the *threshold supersaturation*. We shall also extend this term to mean the actual value of supersaturation at which nucleation can take place when the solution is confined within a porous rock.

Some general principles of the relationship between supersaturation gradients and the threshold supersaturation at nucleation in many salt crystallization systems were determined as a function of cooling rate and have been investigated both experimentally and theoretically (Nyvlt 1968; Nyvlt et al. 1985; Kubota et al. 1978, 1986, 1988). The general relationship between the cooling rate (i.e., supersaturation rate) and the degree of undercooling (threshold supersaturation) is:

$$\text{Supersaturation rate} \propto (\text{Threshold supersaturation})^m$$

or

$$R_{\Omega} = K(\Omega_{\text{th}})^m \quad (3)$$

where K and m are empirical coefficients, and Ω_{th} is the threshold supersaturation.

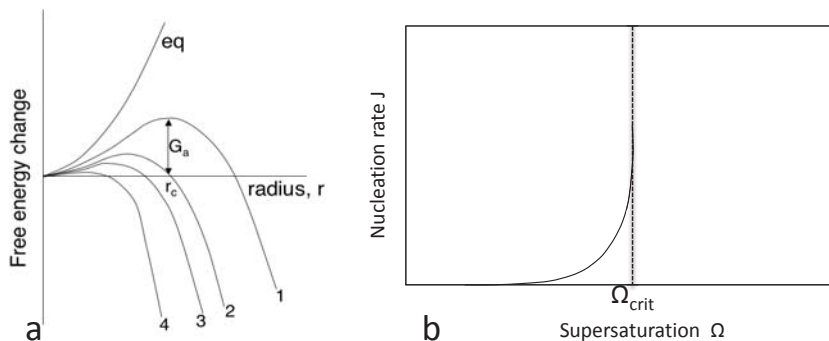


Figure 5. (a) Schematic drawing of the change in free energy as a function of nucleus size according to classical nucleation theory (CNT). The curve “eq” represents the free energy of a particle formed at equilibrium where only a surface energy term would be relevant. Curves (1) to (4) show the situation with increasing supersaturation where the reduction in free energy is dominated by the volume free energy of the nucleus. (b) A consequence of CNT is that the nucleation rate is a very sharp function of the supersaturation and defines an approximate value of the critical supersaturation for nucleation.

Crystallization experiments in confined media

Crystallization of ice. When aqueous solutions are confined to occupy a specific volume, we need to consider additional factors which could contribute to the threshold supersaturation for crystallization. A confined solution could be a droplet in a pore space or a thin film in a grain boundary.

There has been an active interest in crystallization in small droplets for centuries, ever since the observation that liquid fogs and clouds could persist well below the frost point of water. The degree of undercooling possible in small droplets continues to be a subject of intensive research, especially since the radiative properties of ice clouds and the climatic consequences depend on the size of cloud particles. It is well known that small water droplets in clouds can be supercooled to at least -30°C and in some cases as low as -40°C —supercooling, meaning that the water is lowered to that temperature without crystallization as ice (e.g., McDonald 1953; Prupacher 1995). Numerous experiments on the freezing points of ultrapure water droplets have demonstrated an approximately linear dependence of the degree of undercooling on droplet size (Fig. 6) (for a summary see Prupacher 1995). These experiments were designed to measure homogeneous nucleation temperatures. The addition of any particles of impurities or dust would immediately provide seeds and promote heterogeneous nucleation of ice.

However, even for carefully designed experiments to avoid heterogeneous nucleation, the interpretation of the results is made complicated by the presence of the water–air interface, and it has been argued that the nucleation rate at this interface is orders of magnitude faster than within the bulk droplet (Tabazadeh et al. 2002; Shaw et al. 2005). If the interface between the water droplet and its surroundings is an important factor then two opposing effects have to be taken into account: first, according to CNT the nucleation rate at a given supercooling should decrease as the droplet size decreases, but second, a smaller droplet will have a larger surface to volume ratio and hence the surface nucleation rate will increase. For pure water the experimental results suggest that the surface nucleation rate could become comparable to the volume nucleation rate at droplet radii below $\sim 4\ \mu\text{m}$ (Duft and Leisner 2004; Earle et al. 2010).

Ice crystallization at large values of undercooling is made more complex because of the changing viscosity and hydrogen bonding at such low temperatures and further discussion of ice is beyond the scope of this chapter. Nevertheless the ice example illustrates two important points: (i) that the volume of the solution droplet is important, and (ii) that the interface between the solution and its surroundings will also play a role.

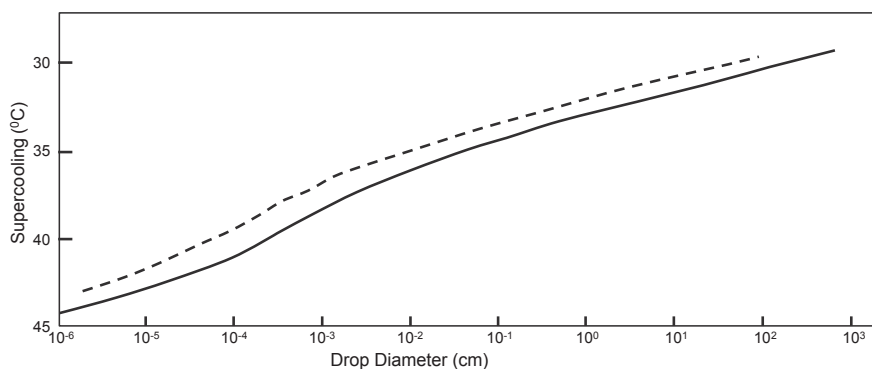


Figure 6. The relationship between the supercooling required to crystallize ice from ultra-pure water, as a function of the drop diameter. The full line is for a cooling rate of $1\ ^{\circ}\text{C}\ \text{s}^{-1}$ and the dashed line for a cooling rate of $1\ ^{\circ}\text{C}\ \text{min}^{-1}$. The data for the lines are from a large number of experiments analyzed by Prupacher (1995).

Crystallization of salts in small pores. Various experimental and theoretical approaches have been applied to the question of threshold supersaturation when an aqueous solution is confined in a porous medium. As well as the need to consider pore size, salt crystallization introduces the need to consider diffusion of ions through a solution to the crystallizing nucleus, and therefore the inevitability of compositional gradients forming around a crystal. As we have noted above, compositional gradients suggest supersaturation gradients in space as well as time and this will have an impact on the threshold supersaturation.

Experiments designed to investigate these effects on the crystallization of sparingly soluble salts have been used by Prieto et al. (1988, 1989, 1990, 1994) and Putnis et al. (1995). The porous medium used is silica hydrogel and crystallization is induced by the counter-diffusion of ions from opposite ends of a diffusion column (Fig. 7). The silica hydrogel contains ~95 vol% of solution within an interconnecting porous network where the pore diameters are typically from 100 to 500 nm although secondary pores of up to 10 μm are also common (Henisch 1988). The gel inhibits advection and convection and transport of ions is purely by diffusion through the pore spaces. It is known that under these circumstances nucleation is inhibited and the threshold supersaturation is high. It is possible to determine the rate of change of supersaturation as well as the actual threshold supersaturation at the point of nucleation within the column (Prieto et al. 1994; Putnis et al. 1995). The results for a number of different salts (Fig. 8) follow the same empirical law that was found in cooling experiments, i.e., that

$$\text{Supersaturation rate} \propto (\text{Threshold supersaturation})^m.$$

Note the wide range of threshold supersaturation depending on the solubility (and hence the surface energy) of the salt, consistent with the expectations from classical nucleation theory. However, the meaning of the slopes of the straight lines in the \ln - \ln plots in Figure 8 is still not well understood (Prieto 2014).

Although these experiments are a good demonstration of the effect of supersaturation rate on the threshold supersaturation, the reason for the suppression of nucleation in the silica hydrogel is not clear. The implication is that it is due to the suppression of advection and convection relative to crystal growth in an open system and that diffusion of the ions through the gel is also reduced due to the small pore size and the tortuosity of the diffusion paths. This hypothesis has been tested by Nindiyasari et al. (2014) in experiments on the growth of CaCO_3 by counter-diffusion in gelatin hydrogels with different pore sizes and porosity distribution.

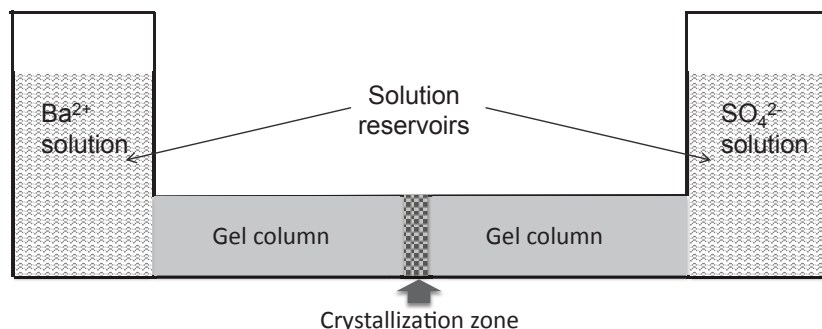


Figure 7. Schematic of the experimental set-up for double diffusion crystal growth experiments where a gel column separates the reacting components, in this case Ba^{2+} and SO_4^{2-} . Counter-diffusion of the components through the gel column eventually supersaturates the fluid and results in precipitation (of BaSO_4 in this case).

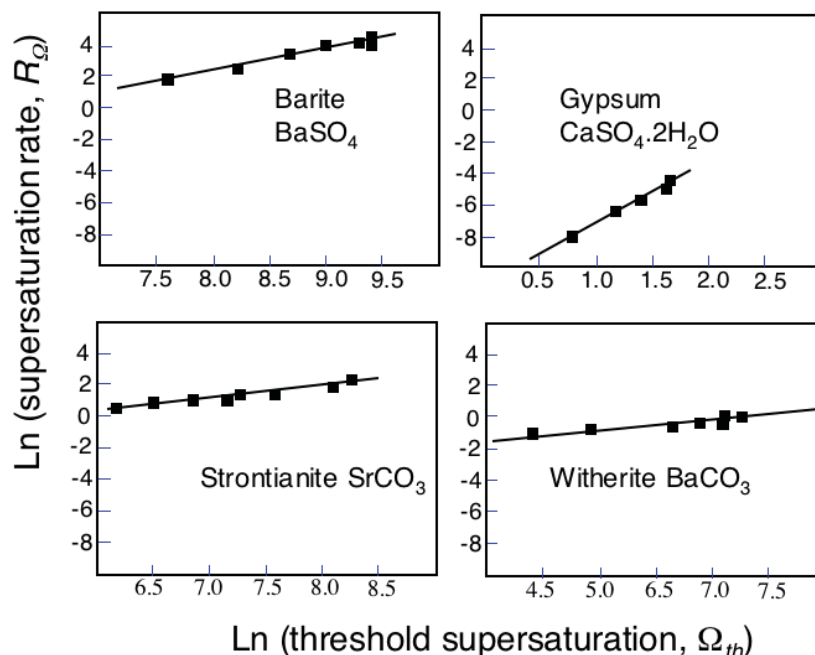


Figure 8. ln–ln plot showing the relationship between the supersaturation rate and the threshold supersaturation for 4 different phases determined from crystallization experiments such as shown in Figure 7 (data from Prieto et al. 1994).

Although the waiting times for nucleation increased significantly and systematically with increasing gelatin content of the gel (and hence reduced total pore volume and pore size), separate diffusion experiments showed that reduced diffusion was not the reason for the inhibition of nucleation in the smaller pore sized gels.

What inhibits nucleation in small pores? A number of possible explanations have been advanced for the observation that nucleation is inhibited in small pores:

(i) Nucleation is a stochastic process that involves random collisions between ions to form clusters. In classical nucleation theory these clusters need to grow to a critical size where the gain in surface energy of the cluster is counterbalanced by the volume reduction in free energy due to forming the solid from a supersaturated solution (Fig. 5a). In the case of sparingly soluble salts, the probability of these random collisions will be small because the number of ions in a given volume is small, even when the supersaturation is high. The induction time is an important feature of classical nucleation theory and is the time between the creation of the supersaturation and the detection of nucleation. The induction time t_i is given by:

$$t_i = 1 / JV \quad (4)$$

where J is the nucleation rate and V is the volume of the solution. At the detection of nucleation, the nucleation rate is taken to be one nucleus in the given volume at the induction time t_i .

Using the standard equations from classical nucleation theory (Kashchiev 2000; Kashchiev and Rosmalen 2003), Prieto (2014) has calculated the supersaturation and induction times for barite precipitation as a function of pore size, assuming that in the nucleation equations the relevant volume V is the volume of a single pore. Figure 9 from Prieto (2014) shows the calculated critical supersaturation and induction times calculated for pore sizes of 0.1 μm and 1 μm ; these were compared to the experimental values from the gel experiments of Prieto et al. (1994) and Putnis et al. (1995). Although there is always some uncertainty about the relevant values of the parameters used in the calculations, the results show a clear dependence of

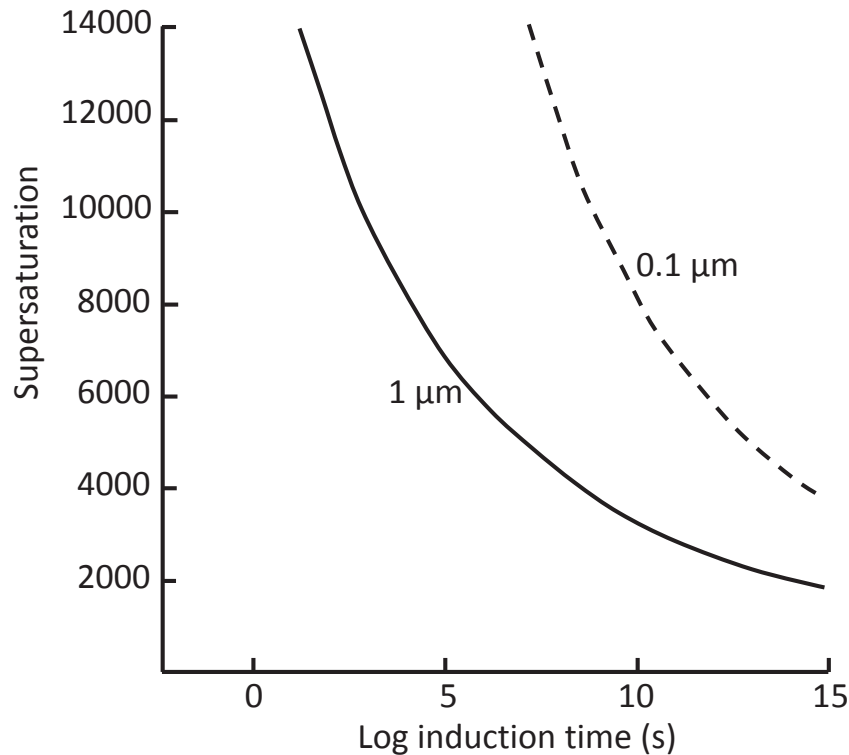


Figure 9. Calculated curves from CNT for the relationship between the supersaturation and the induction time for nucleation in pores of size 0.1 μm and 1 μm (after Prieto 2014).

critical supersaturation on the pore size. These results are also consistent with the experimental observations by Nindiyasari et al. (2014) that higher supersaturation values are needed for crystallization from solutions confined to smaller pores.

(ii) For crystal growth in small pores the crystal size will be limited by the pore size and crystals whose geometry is characterized by a large surface to volume ratio will have a higher solubility than the bulk solubility. Pore-size-controlled solubility (PCS) has been advanced by Emmanuel and Berkowitz (2007), Emmanuel and Ague (2009) and Emmanuel et al. (2010) as an explanation for the preferential precipitation of salts in larger pore volumes. When the effects of surface energy are taken into account, it is possible that a solution could be undersaturated in small pores while being supersaturated in large pores.

Determining the solubility of crystals in small pores is experimentally difficult. One method which has successfully been used to measure the composition of solutions at the point of nucleation or dissolution inside a pore, as well as determining the pore size, is nuclear magnetic resonance spectroscopy (NMR). For Na in solution, the intensity of the NMR peaks can be correlated with solution composition and the relaxation rate to the pore size (Rijniers et al. 2004, 2005). Therefore for Na salts it is possible to determine the solubility as a function of pore size. For Na_2CO_3 , Rijniers et al. (2005) found that the solubility inside 30-nm-sized pores hardly differs from bulk solubility whereas for 10-nm pores the solubility was more than twice the bulk solubility.

According to Espinoza-Marzal and Scherer (2010), PCS needs to be taken into account in pores smaller than 0.1 μm , although the effect of pore size on solubility will be greater for sparingly soluble salts which have a higher surface energy. PCS is likely to be an important factor when considering precipitation in pores in the submicron range (Emmanuel and Ague

2010). Therefore, PCS is another possible explanation for the high threshold supersaturation required to nucleate salts in the gel experiments described above.

(iii) The role of the pore surface. Neither of the previous two possible explanations for the effect of pore size on threshold supersaturation consider the role of the pore wall itself. To test whether the surface chemistry of the pores controlled CaCO_3 precipitation, Stack et al. (2014) introduced supersaturated solutions into a manufactured controlled-pore glass (CPG) which contained both macropores (~32 nm) and nanopores (~8 nm). In some experiments the pore walls were functionalized with a monolayer of anhydride with a polar functional group. Precipitation was studied *in situ* using small angle X-ray scattering, a non-destructive method which allows the researcher to discriminate between different densities in a sample, as well as *ex situ* by scanning transmission electron microscopy. The results showed that in the native CPG, precipitation only took place in the macropores, whereas in the functionalized CPG, precipitation also took place in nanopores, suggesting that a favorable surface chemistry could promote nucleation, even in nanopores.

As mentioned above, the Emmanuel and Berkowitz (2007) model for pore-size-controlled solubility may be relevant for nanometer-sized pores, but not for pores with sizes of several microns. Mürmann et al. (2013) modified this model by considering that the surface charge on the pore walls will interact with the ions in the fluid and change their activity and hence the supersaturation of the fluid. Using a numerical simulation they calculated the relationship between pore size and the crystallization as a function of supersaturation and showed that by including the surface charge the pore radius at which pore-size-controlled solubility is relevant is shifted from the nanometre to the micrometre range. The model could also be relevant to the observations in Stack et al. (2014), where a polar functional group modifies the surface charges on the pore walls and enhances nucleation, although the interpretation of the enhancement in that case involves matching of the crystal structure with the substrate (Lee et al. 2013), rather than the surface charge modifying ion activities.

(iv) The nucleation mechanism. Most interpretations of crystal growth in pores have assumed a classical model of nucleation, i.e., that crystallization first involves the formation of a critical nucleus and then grows by adding further growth units to the cluster. However, such an equilibrium model of balancing positive surface energy terms with negative free energy reduction for nucleation is not likely to be relevant to a situation where nucleation takes place at very high values of supersaturation, as is the case in small pores. Furthermore, there is increasing evidence that even at moderate supersaturation a “non-classical” model of crystal growth involving the oriented attachment and assembly of sub-critical clusters can better explain experimental observations (Niederberger and Cölfen 2006; Gebauer and Cölfen 2011; De Yoreo 2013).

The morphology of crystals grown at high supersaturations in hydrogels also suggests a non-classical nucleation model in which larger crystals are made up by the oriented attachment of smaller crystallites (e.g., Grassmann et al. 2003; Nindiyasari et al. 2014). Nindiyasari et al. (2014) also noted that the mosaic spread of calcite aggregates grown in gels increases when the pore size is smaller. In the non-classical model, pre-nucleation nanoclusters exist in supersaturated solutions effectively reducing the activity of the ions in solution. Thus the concepts we use to define supersaturation at the point of crystal growth would need to be redefined.

DISCUSSION

In a geological context, the evolution of porosity, its generation and destruction through fluid–mineral interaction is of utmost importance. In a sedimentary basin undergoing diagenesis, for example, compaction processes reduce the primary porosity in an unconsolidated sediment through pressure solution and reprecipitation of material into the pore spaces. At the same time, increasing temperature and pressure will induce porosity-generating reactions between saline solutions and the minerals in the sediment. We have seen how porosity generation is an integral aspect of the re-equilibration of a rock by interface-coupled dissolution–precipitation, but that this porosity is also a transient feature which may be annihilated by recrystallisation. Even when porosity is preserved as is the case in the albitized feldspar in Figure 3a, permeability can be drastically reduced if the pores lose connectivity. This effectively closes the mineral to further fluid flow and the pores are preserved as fluid inclusions.

As long as fluid flow through a porous rock is still possible, the pore spaces serve as sites for crystal growth, further reducing the porosity and potentially clogging the rock. The reduction of permeability has obvious consequences for the extraction of fluids from a rock as in oil and gas recovery and in geothermal reservoirs. It is therefore important to understand the factors which control such secondary mineralization and pore size appears to be a major factor controlling nucleation and growth.

In this final section we give some further examples of the role of pore size on crystallization and its consequences and interpret these in terms of the experimental results quoted above.

(i) The porous sandstones of the Lower Triassic Bunter Formation in north-west Germany have been studied as potential reservoir rocks for gas storage. However, due to the proximity of salt domes the pore fluids are highly saline and salt cementation in the pore space significantly deteriorates the reservoir quality, reducing the porosity from ~30% to 5% and the permeability by up to 4 orders of magnitude (Putnis and Mauthe 2001). In some parts of this Formation the sandstone has small scale (~1 mm) periodic variations in grain size, allowing a study of the effect of pore size on halite precipitation (Putnis and Mauthe 2001). Figure 10 shows an

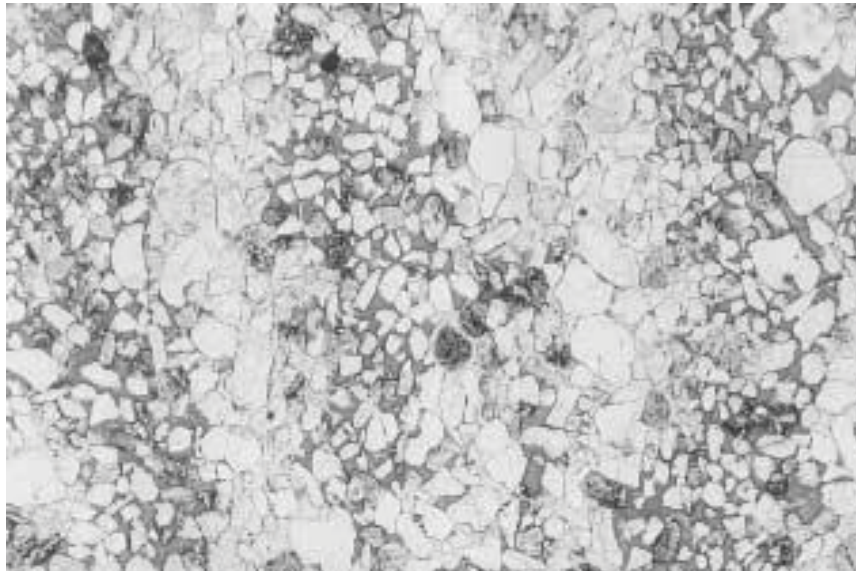


Figure 10. Micrograph of a thin section of a sandstone, with a periodic variation of quartz grain size, which has been partly cemented by halite (NaCl). The sandstone has subsequently been injected with a dark resin which reveals the residual porosity. The unfilled pores are all in the finer grain size sandstone while the larger pores between the coarser grains have been fully cemented by halite. The width of the micrograph is 4.2 mm.

optical micrograph of such a sandstone sample in which the residual porosity is shown by the dark resin which is injected into the sample before preparing the thin section. The resin only penetrates the finer sandstone layers, as the coarser layers are fully cemented with halite.

Quantitative measurements of the pore size distributions in these rocks showed that the size of the pores left uncemented by salt is decreased as the porosity and permeability is reduced, so that the first pores to be salt-cemented were the largest with pore diameters in the tens of micron range. Progressively smaller pores are filled until the residual pore size in the most cemented samples is submicron.

If we assume that the NaCl concentration in solution was uniform throughout (but see below), our conclusion would be that the solution in the small pores was able to maintain a higher supersaturation before crystallization, compared to the larger pores. The persistence of open pores in the submicron range could be the result of pore-size controlled solubility, but this does not explain the differences when the pore sizes are much larger. Some other systematic effect of surface to volume ratio of the pores, such as the surface-charge model suggested by Mürmann et al. (2013) or effects related to solute transport into pores of different sizes may be important.

A similar permeability reduction problem has afflicted the development of a geothermal plant within the Upper Triassic Rhaetian sandstone succession in northern Germany, where anhydrite precipitation has effectively reduced the flow of hot water below that needed to be economic (Wagner et al. 2005). Analysis of core samples showed that anhydrite precipitation was restricted to regions of relatively high primary porosity, while regions of low porosity remained uncemented.

In the discussion so far the assumption has been that the solute concentration in pore fluid throughout the pore-space of a rock is homogeneous and that the same concentration of solute could result in solution in large pores being supersaturated while that in small pores was undersaturated. However, this is likely to be an oversimplification particularly as the layer of a reactive fluid in contact with a mineral surface is different from the bulk composition (Putnis et al. 2005; Ruiz-Agudo et al. 2012). Therefore, the definition of ‘bulk’ in this context would depend on pore size. Sequential centrifugation has been widely used to extract pore water from a rock and it has been demonstrated that with increasing centrifugal speed water is progressively extracted first from larger pores and then from smaller pores (Edmunds and Bath 1976). Therefore, changing solution concentrations expelled from a rock with increasing centrifugal speed have been interpreted as an indication that larger pores have different solute concentrations than small pores and that concentration gradients exist in reacting rocks (Yokoyama et al. 2011 and references therein). The fact that reactive fluid infiltration into a rock is a heterogeneous phenomenon depending on local flow paths is a commonplace observation with implications for local rock strength, deformation, and differential stress (Mukai et al. 2014; Wheeler 2014).

(ii) Salt crystallization in porous rocks—weathering and disintegration. The relationship between pore size and threshold supersaturation for crystal growth has dramatic consequences when salts grow in the pores of rock and concrete. Confined crystals growing from a supersaturated solution exert a stress (crystallization pressure) on the pore walls through a thin film of supersaturated fluid between the crystal and the pore wall (Steiger 2005a,b). Supersaturation may be generated through evaporation so the point at which a solution reaches the threshold supersaturation will determine the size of the crystallization pressure. Rapid evaporation increases the supersaturation rate and hence the threshold supersaturation. The presence of small pores, in which the threshold supersaturation can be very high, results in greater damage during fluid evaporation. Repeated wetting and drying of salt solutions generates sufficient damage to eventually disintegrate sandstone, limestone, and concrete.

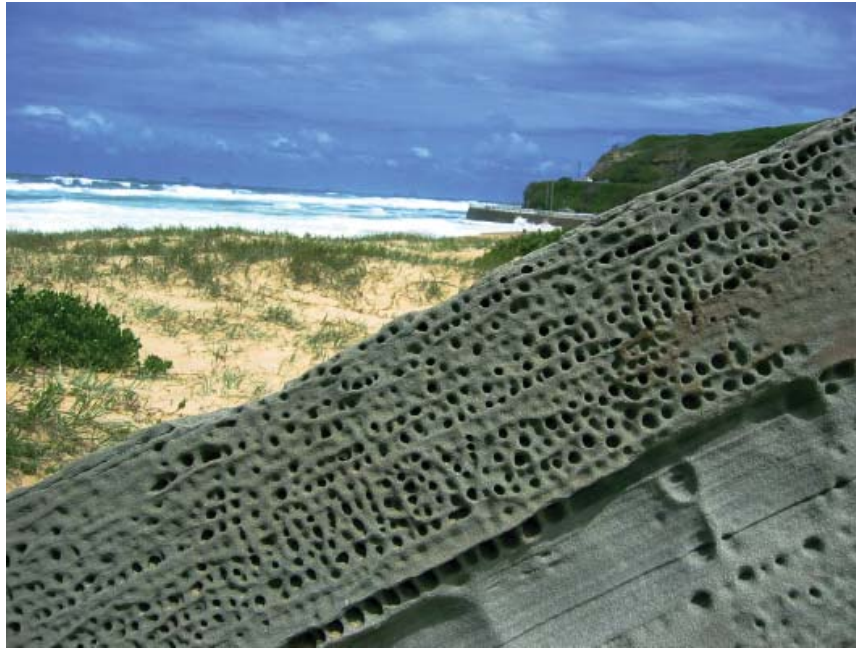


Figure 11. Photograph of honeycomb weathering in sandstone, Nobby's Beach, Newcastle, Australia.

Salts with high surface energy such as the sodium sulfate hydrates require high values of supersaturation to nucleate and so are capable of causing the greatest damage, whereas halite has always been considered as having a very high nucleation rate even at low supersaturation. However, the very common phenomenon of honeycomb weathering of rocks in coastal environments (Fig. 11) and deserts with saline groundwater suggests that even halite crystallization in porous rocks enhances weathering and erosion (Wellman and Wilson 1965; Rodriguez-Navarro et al. 1999b; Doehne 2002). Recent work on NaCl crystallization in solutions confined in microcapillaries (Desarnaud et al. 2014) has shown that nucleation takes place at considerably higher values of supersaturation than previously assumed, at $S \sim 1.6$ where S is defined as the ratio of concentration relative to the bulk solubility value. At such a high value the crystallization pressure would be more than sufficient to exceed the tensile strength of sedimentary rocks (Derluyn et al. 2014).

(iii) Mineral vein formation involves the supersaturation of an aqueous solution and subsequent precipitation in a narrow dilatational feature in a rock. Because the veins form after the formation of the host rock, the vein characteristics and the microstructures of the minerals within the vein have been used to provide information about paleo-stress fields, deformation mechanisms which may have caused the dilatation as well as fluid pathways (Bons et al. 2012). Vein formation is ultimately related to the formation of fractures in a rock, and fracture mechanics is a topic beyond the scope of this chapter (but see Røyne and Jamtveit 2015, this volume). However the generation of supersaturation does relate to some of the issues discussed here.

There are a number of ways that supersaturation can be generated, and the most commonly discussed are changes in temperature and pressure, which reduce the solubility of a mineral, changes in the chemical environment, such as pH and Eh (redox conditions), and fluid mixing and changes in composition of a fluid due to interaction with the host rock. These factors have been reviewed by Bons et al. (2012). However, another rarely mentioned possibility is that diffusional and advective transport of material and fluid from the pores in the bulk rock into a dilatational feature will initiate supersaturation due to the fact that an open space cannot

sustain the same level of supersaturation as in the small pores in a rock (Putnis et al. 1995). In such a case the fluid transport may be normal to the vein rather than fluid flow along an open fracture (Fisher and Brantley 1992; Fisher et al. 1995) and equilibrium solubility values would not be relevant in determining the amount of fluid required to precipitate a given amount of vein material. In such veins, the mineral growth originates from a small fracture which then forms a median line within the vein as the fracture widens. The mineral growth is then from this median line towards the vein wall (antiaxial) compared with mineral growth in an open fracture which starts from the walls and grows inwards (syntaxial). The various styles of vein formation and the mineral microstructures associated with different types of veins have been discussed by Elburg et al. (2002) and Bons et al. (2012).

CONCLUSIONS

Although the fundamental origin of the relationship between pore size and fluid supersaturation is still not totally understood, and may be the result of a number of interacting parameters, there is no doubt that the pore structure exerts a very significant influence on every aspect of crystal growth. In sedimentary rocks undergoing diagenesis, porosity generation through fluid–mineral re-equilibration with increasing T , P is contemporaneous with porosity destruction through compaction and recrystallization. The interplay between these processes will form a lively topic of research for years to come. Similarly, in low permeability crystalline rocks the feedback is between reaction-driven porosity generation and which allows further fluid infiltration providing the mechanism for large-scale metamorphic and metasomatic reactions.

ACKNOWLEDGMENTS

The early experiments on the generation of porosity during salt replacement by Christine V. Putnis, University of Münster and her colleagues led to the development of our understanding of mineral replacement mechanisms, and then together with Håkon Austrheim and Bjørn Jamtveit, University of Oslo to the wider applications to fluid-rock interaction. Many of the concepts relating to supersaturation in porous media have been developed through many years of discussions with Manuel Prieto, University of Oviedo. I thank Sue Brantley and Carl Steefel for comments that have improved this chapter. Financial support from the Marie Curie-Sklodowska Action of the European Union (FlowTrans: Flow and Transformation in Porous Media PITN-GA-2012-316889) is gratefully acknowledged.

REFERENCES

- Bjørlykke K (2014) Relationships between depositional environments, burial history and rock properties. Some principal aspects of diagenetic process in sedimentary basins. *Sed Geol* 301:1–14
- Boles JR (1982) Active albitization of plagioclase, Gulf Coast Territory. *Am J Sci* 282:165–180
- Bons PD, Elburg MA, Gomez-Rivas E (2012) A review of the formation of tectonic veins and their microstructures. *J Struct Geol* 43:33–62
- Buss H, Sak P, Webb RM, Brantley S (2008) Weathering of the Rio Blanco quartz diorite, Luquillo Mountains, Puerto Rico: Coupling oxidation, dissolution and fracturing. *Geochim Cosmochim Acta* 72:4488–4507
- Dalby KN, Anderson AJ, Mariano AN, Gordeon RA, Mayanovic RA, Wirth R (2010) An investigation of cathodoluminescence in albite from the A-type Georgeville granite, Nova Scotia. *Lithos* 114:86–94
- Derluyn H, Moonen P, Carmeliet J (2014) Deformation and damage due to drying induced crystallization in porous limestone. *J Mech Phys Solids* 63:242–255
- Desarnaud J, Derluyn H, Carmeliet J, Bonn D, Shahidzadeh N (2014) Metastability limit for the nucleation of NaCl crystals in confinement. *J Phys Chem Lett* 5:890–895
- De Yoreo J (2013) Crystal nucleation: more than one pathway. *Nature Mater* 12:284–285

- Doehne E (2002) Salt weathering: a selective review. *In*: Siegesmund S, Weiss T, Vollbrecht A (eds) *Natural Stones, Weathering Phenomena, Conservation Strategies and Case Studies*. Geol Soc Spec Publ 205:43–56
- Dohmen R, Milke R (2010) Diffusion in polycrystalline materials: grain boundaries, mathematical models and experimental data. *Rev Mineral Geochem* 72:921–970
- Duft D, Leisner T (2004) Laboratory evidence for volume-dominated nucleation of ice in supercooled water microdroplets. *Atmos Phys Chem* 4:1997–2000
- Earle ME, Kuhn T, Khalizov AF, Sloan JJ (2010) Volume nucleation rates for homogeneous freezing in supercooled water droplets: results from a combined experimental and modelling approach. *Atmos Chem Phys* 10:7945–7961
- Edmunds WM, Bath AH (1976) Centrifuge extraction and chemical analysis of interstitial waters. *Environ Sci Technol* 10:467–472
- Elburg MA, Bons PD, Foden J, Passchier CW (2002) The origin of fibrous veins: constraints from geochemistry. *Geol Soc Spec Publ* 200:103–118
- Emmanuel S, Ague JJ (2009) Modeling the impact of nano-pores on mineralization in sedimentary rocks. *Water Resour Res* 45:W04406
- Emmanuel S, Berkowitz B (2007) Effects of pore-size controlled solubility on reactive transport in heterogeneous rock. *Geophys Res Lett* 34:L06404
- Emmanuel S, Ague JJ, Walderhaug O (2010) Interfacial energy effects and the evolution of pore size distributions during quartz precipitation in sandstone. *Geochim Cosmochim Acta* 74:3539–3552
- Engvik AK, Putnis A, FitzGerald JD, Austrheim H (2008) Albitization of granitic rocks: the mechanism of replacement of oligoclase by albite. *Can Mineral* 46:1401–1415
- Espinoza-Marzal RM, Scherer G (2010) Advances in understanding damage by salt crystallization. *Accounts Chem Res* 43:897–905
- Fisher DM, Brantley SL (1992) Models of quartz overgrowth and vein formation: deformation and episodic fluid flow in an ancient subduction zone. *J Geophys Res* 97:20043–20061
- Fisher DM, Brantley SL, Everett M, Dzvoniak J (1995) Cyclic fluid flow through a regionally extensive fracture network within the Kodiak accretionary prism. *J Geophys Res* 100:12881–12894
- Fletcher RC, Buss H, Brantley SL (2006) A spheroidal weathering model coupling porewater chemistry to soil thicknesses during steady-state denudation. *Earth Planet Sci Lett* 244:444–457
- Folk RL (1955) Note on the significance of “turbid” feldspars. *Am Mineral* 40:356–357
- Gebauer D, Cölfen H (2011) Prenucleation clusters and non-classical nucleation. *Nano Today* 6:564–584
- Grassmann O, Neder RB, Putnis A, Löbmann P (2003) Biomimetic control of crystal assembly by growth in an organic hydrogel network. *Am Mineral* 88:647–652
- Gratier J-P, Dysthe DK and Renard F (2013) The role of pressure solution creep in the ductility of the Earth’s upper crust. *Adv Geophys* 54:47–179
- Guthrie GD, Veblen DR (1991) Turbid alkali feldspars from the Isle of Skye, northwest Scotland. *Contrib Mineral Petrol* 108:298–304
- Harlov DE, Hansen EC, Bigler C (1998) Petrologic evidence for K-feldspar metasomatism in granulite facies rocks. *Chem Geol* 151:373–386
- Henisch HK (1988) *Crystals in Gels and Liesegang Rings*. Cambridge University Press, Cambridge
- Hövelmann J, Putnis A, Geisler T, Schmidt B, Golla-Schindler U (2010) The replacement of plagioclase feldspars by albite: observations from hydrothermal experiments. *Contrib Mineral Petrol* 159:43–59
- Iyer K, Jamtveit B, Mathiesen J, Malthe-Sørenssen A, Feder J (2008) Reaction-assisted hierarchical fracturing during serpentinization. *Earth Planet Sci Lett* 267:503–516
- Jamtveit B, Yardley B (1997) *Fluid Flow and Transport in Rocks*. Chapman & Hall, London
- Jamtveit B, Putnis CV, Malthe-Sørenssen A (2009) Reaction induced fracturing during replacement processes. *Contrib Mineral Petrol* 157:127–133
- Janssen A, Putnis A, Geisler T, Putnis CV (2010) The experimental replacement of ilmenite by rutile in HCl solutions. *Mineral Mag* 74:633–644
- Kashchiev D (2000) *Nucleation: Basic Theory with Applications*. Butterworth-Heinemann, Oxford
- Kashchiev D, van Rosmalen GM (2003) Review: Nucleation in solutions revisited. *Crystal Res Technol* 38:555–574
- Kasioptas A, Geisler T, Perdikouri C, Trepmann C, Gussone N, Putnis A (2011) Polycrystalline apatite synthesised by hydrothermal replacement of calcium carbonates. *Geochim Cosmochim Acta* 75:3486–3500
- Kubota N, Karasawa H, Kawakami T (1978) On estimation of critical supercooling from waiting times measured at constant supercooling. *J Chem Eng Jpn* 11:290–295
- Kubota N, Kawakami T, Tadaki T (1986) Calculation of supercooling temperature for primary nucleation of potassium nitrate from aqueous solution by the two-kind active site model. *J Cryst Growth* 74:259–274

- Kubota N, Fujisawa Y, Tadaki T (1988) Effect of volume on the supercooling temperature for primary nucleation of potassium nitrate from aqueous solution. *J Cryst Growth* 89:545–552
- Laporte D, Watson EB (1991) Direct observation of near-equilibrium pore geometry in synthetic quartzites at 600–8000 °C and 2–10.5 kbar. *J Geol* 99:873–878
- Lee VW, Mackwell SJ, Brantley SL (1991) The effect of fluid chemistry on wetting textures in novaculite. *J Geophys Res* 96:10023–10037
- Lee JI, Lee YI (1998) Feldspar albitization in Cretaceous non-marine mudrocks, Gyeongsang Basin, Korea. *Sediment* 45:745–754
- Lee MR, Parsons I (1997) Dislocation formation and albitization in alkali feldspars from the Shap Granite. *Am Mineral* 82:557–570
- Lee JRI, Han TY-J, Willey TM, Nielsen MH, Klivamsky LM, Liu Y, Chung S, Terminello LJ, van Buuren T, de Yoreo JJ (2013) Cooperative reorganization of mineral and template during directed nucleation of calcium carbonate. *J Phys Chem C* 117:11076–11085
- Martin RF, Bowden P (1981) Peraluminous granites produced by rock-fluid interaction in the Ririwai nonorogenic Ting-complex, Nigeria: mineralogical evidence. *Can Mineral* 19:65–82
- McDonald JE (1953) Homogeneous nucleation of supercooled water drops. *J Meteorol* 10:416–433
- Merino E (1975) Diagenesis in Tertiary sandstones from Kettleman North Dome, California: I. Diagenetic mineralogy. *J Sed Petrol* 45:320–336
- Milke R, Neusser G, Kolzer K, Wunder B (2013) Very little water is necessary to make a dry solid silicate system wet. *Geology* 41:247–250
- Montgomery CW, Brace WF (1975) Micropores in plagioclase. *Contrib Mineral Petrol* 52:17–28
- Mukai H, Austrheim H, Putnis CV, Putnis A (2014) Textural evolution of plagioclase feldspar across a shear zone: implications for deformation mechanism and rock strength. *J Petrol* 55:1457–1477
- Mürmann M, Kühn M, Pape H, Clauser C (2013) Numerical simulation of pore size dependent precipitation in geothermal reservoirs. *Energy Procedia* 40:107–116
- Navarre-Sitchler A, Brantley SL, Rother G (2015) How porosity increases during incipient weathering of crystalline silicate rocks. *Rev Mineral Geochem* 80:331–354
- Niederberger M, Cölfen H (2006) Oriented attachment and mesocrystals: Non-classical crystallization mechanisms based on nanoparticle assembly. *Phys Chem Chem Phys* 8:3271–3287
- Niedermeier DRD, Putnis A, Geisler T, Golla-Schindler U, Putnis CV (2009) The mechanism of cation and oxygen isotope exchange in alkali feldspars under hydrothermal conditions. *Contrib Mineral Petrol* 157:65–76
- Nielsen AE (1967) Nucleation in aqueous solution. *J Phys Chem Solids suppl.* 1:419–426
- Nijland TG, Harlov DE, Andersen T (2014) The Bamble Sector, south Norway: A review. *Geoscience Frontiers* 5:635–658
- Nindiyasari F, Fernández-Díaz L, Griesshaber E, Astilleros JM, Sánchez-Pastor N, Schmahl WW (2014) Influence of gelatin hydrogel porosity on the crystallization of CaCO₃. *Cryst Growth Des* 14:1531–1542
- Norberg N, Neusser G, Wirth R, Harlov D (2011) Microstructural evolution during experimental albitization of K-rich alkali feldspar. *Contrib Mineral Petrol* 162:531–546
- Norberg N, Harlov D, Neusser G, Wirth R, Rhede D, Morales L (2013) Experimental development of patch perthite from synthetic cryptoperthite: Microstructural evolution and chemical re-equilibration. *Am Mineral* 98:1429–1441
- Nyvtl J (1968) Kinetics of nucleation in solutions. *J Crystal Growth* 3:377–383
- Nyvtl J, Söhnle O, Matuchova M, Broul M (1985) *The Kinetics of Industrial Crystallization*. Elsevier, Amsterdam
- Ozawa H (1997) Thermodynamics of frost heaving: A thermodynamic proposition for dynamic phenomena. *Phys Rev E* 56:2811–2816
- Parnell J (ed) (1998) *Dating and duration of fluid flow and fluid-rock interaction*. Geol Soc Spec Publ 144
- Parsons I (1978) Feldspars and fluid in cooling plutons. *Mineral Mag* 42:1–17
- Parsons I, Lee MR (2009) Mutual replacement reactions in alkali feldspars I: microtextures and mechanisms. *Contrib Mineral Petrol* 157:641–661
- Perdikouri C, Kasiotas A, Geisler T, Schmidt BC, Putnis A (2011) Experimental study of the aragonite to calcite transition in aqueous solution. *Geochim Cosmochim Acta* 75:6211–6224
- Perez R, Boles AR (2005) An empirically derived kinetic model for albitization of detrital plagioclase. *Am J Sci* 305:312–343
- Plümper O, Putnis A (2009) The complex hydrothermal history of granitic rocks: multiple feldspar replacement reactions under subsolidus conditions. *J Petrol* 50:967–987
- Pollok K, Putnis CV, Putnis A (2011) Mineral replacement reactions in solid solution-aqueous solution systems: Volume changes, reactions paths and end-points using the example of model salt systems. *Am J Sci* 311:211–236

- Prieto M (2014) Nucleation and supersaturation in porous media (revisited). *Mineral Mag* 78:1437–1447 doi: 10.1180/minmag.2014.078.6.11
- Prieto M, Viedma C, Lopez-Aceueodo V, Martin-Vivaldi JL, Lopez-Andres S (1988) Mass transfer and supersaturation in crystal growth in gels. Application to $\text{CaSO}_4 \cdot 2\text{H}_2\text{O}$. *J Cryst Growth* 92:61–68
- Prieto M, Fernández-Díaz L, Lopez-Andres S (1989) Supersaturation evolution and first precipitate location in crystal growth in gels; application to barium and strontium carbonates. *J Cryst Growth* 98:447–460
- Prieto M, Putnis A, Fernández-Díaz L (1990) Factors controlling the kinetics of crystallization: supersaturation evolution in a porous medium. Application to barite crystallization. *Geol Mag* 127:485–495
- Prieto M, Putnis A, Fernández-Díaz L, Lopez-Andres S (1994) Metastability in diffusing-reacting systems. *J Cryst Growth* 142:225–235
- Pruppacher HR (1995) A new look at homogeneous ice nucleation in supercooled water drops. *J Atmos Sci* 52:1924–1933
- Putnis A (2002) Mineral replacement reactions: from macroscopic observations to microscopic mechanisms. *Mineral Mag* 66:689–708
- Putnis A (2009) Mineral replacement reactions. *Rev Mineral Geochem* 30:87–124
- Putnis A, Austrheim H (2010) Fluid induced processes: Metasomatism and Metamorphism. *Geofluids* 10:254–269
- Putnis A, Austrheim H (2012) Mechanisms of metasomatism and metamorphism on the local mineral scale: The role of dissolution–reprecipitation during mineral reequilibration. *In: Metasomatism and the Chemical Transformation of Rock*. Harlov DE and Austrheim H (eds). Springer-Verlag, Berlin, p 139–167
- Putnis A, John T (2010) Replacement processes in the Earth's Crust. *Elements* 6:159–164
- Putnis A, Mauthe G (2001) The effect of pore size on cementation in porous rocks. *Geofluids* 1:37–41
- Putnis CV, Mezger K (2004) A mechanism of mineral replacement: isotope tracing in the model system $\text{KCl-KBr-H}_2\text{O}$. *Geochim Cosmochim Acta* 68:2839–2848
- Putnis A, Putnis CV (2007) The mechanism of reequilibration of solids in the presence of a fluid phase. *J Solid State Chem* 180:1783–1786
- Putnis A, Prieto M, Fernández-Díaz L (1995) Fluid supersaturation and crystallization in porous media. *Geol Mag* 132:1–13
- Putnis CV, Tsukamoto K, Nashimura Y (2005) Direct observation of pseudomorphism: Compositional and textural evolution at a solid–fluid interface. *Am Mineral* 90:1902–1912
- Putnis A, Hinrichs R, Putnis CV, Golla-Schindler U, Collins L (2007) Hematite in porous red-clouded feldspars: evidence of large-scale crustal fluid–rock interaction. *Lithos* 95:10–18
- Raufaste C, Jamtveit B, John T, Meakin P, Dysthe D (2011) The mechanism of porosity formation during solvent-mediated phase transformations. *Proc R Soc Math Phys Eng Sci* 467:1408–1426
- Renard F, Ortoleva P, Gratier JP (2007) Pressure solution in sandstones: influence of clays and dependence on temperature and stress. *Tectonophys* 280:257–266
- Rijniers LA, Magusin PCMM, Huinink HP, Pel L, Kopinga K (2004) Sodium NMR relaxation in porous materials. *J Mag Res* 167:25–30
- Rijniers LA, Huinink HP, Pel L, Kopinga K (2005) Experimental evidence of crystallization pressure inside porous media. *Phys Rev Lett* 94:075503
- Rodriguez-Navarro C, Doehne E (1999a) Salt weathering: Influence of evaporation rate, supersaturation and crystallization pattern. *Earth Surf Proc and Landf* 24:191–209
- Rodriguez-Navarro C, Doehne E, Sebastian E (1999b) Origins of honeycomb weathering: The role of salts and wind. *Geol Soc Am Bull* 111:1250–1255
- Røyne A, Jamtveit B (2015) Pore-scale controls on reaction. *Rev Mineral Geochem* 80:25–44
- Røyne A, Jamtveit B, Malthe-Sørensen A (2008) Controls on weathering rates by reaction-induced hierarchical fracturing. *Earth Planet Sci Lett* 275:364–369
- Ruiz-Agudo E, Putnis CV, Rodriguez-Navarro C, Putnis, A (2012) The mechanism of leached layer formation during chemical weathering of silicate minerals. *Geol* 40:47–950
- Ruiz-Agudo E, Putnis CV, Putnis A (2014) Coupled dissolution and precipitation at mineral–fluid interfaces. *Chem Geol* 383:132–146
- Rutter EH (1983) Pressure solution in nature, theory and experiment. *J Geol Soc* 140:725–740
- Scherer GW (1999) Crystallization in pores. *Cem Concr Res* 34:1613–1624
- Schermerhorn LJG (1956) The granites of Trancoso (Portugal): a study in microclinization. *Am J Sci* 254:329–348
- Shaw RA, Durant AJ, Mi Y (2005) Heterogeneous surface crystallization observed in undercooled water. *J Phys Chem B* 109:9865–9868
- Stack AG, Fernandez-Martinez A, Allard LF, Banuelos JL, Rother G, Anovitz LM, Cole DR, Waychunas GA (2014) Pore-size dependent calcium carbonate precipitation controlled by surface chemistry. *Environ Sci Technol* 48:6177–6183
- Steiger M (2005a) Crystal growth in porous materials I: The crystallization pressure of large crystals. *J Cryst Growth* 282:455–469

- Steiger M (2005b) Crystal growth in porous materials II: Influence of crystal size on crystallization pressure. *J Cryst Growth* 282:470–481
- Tabazadeh A, Djikaev YS, Reiss H (2002) Surface crystallization of supercooled water in clouds. *PNAS* 99:15873–15878
- Velbel MA (1993) Formation of protective surface layers during silicate-mineral weathering under well-leached, oxidizing conditions. *Am Mineral* 78:405–414
- von Bargen N, Waff HS (1986) Permeabilities, interfacial areas and curvatures of partially molten systems: Results of numerical computations of equilibrium microstructures. *J Geophys Res* 91:9261–9276
- Wagner R, Kühn M, Meyn V, Pape H, Vath U, Clauser C (2005) Numerical simulation of pore space clogging in geothermal reservoirs by precipitation of anhydrite. *Int J Rock Mech Min Sci* 42:1070–1081
- Waldron KA, Parsons I, Brown WL (1993) Solution–redeposition and the orthoclase–microcline transformation: evidence from granulites and relevance to ^{18}O exchange. *Mineral Mag* 57:687–695
- Walker FDL (1990) Ion microprobe study of intragrain micropermeability in alkali feldspars. *Contrib Mineral Petrol* 106:124–128
- Walker FDL, Lee MR, Parsons I (1995) Micropores and micropermeable texture in alkali feldspars: geochemical and geophysical implications. *Mineral Mag* 59:505–534
- Walther JV, Wood BJ (1984) Rate and mechanism in prograde metamorphism. *Contrib Mineral Petrol* 88:246–259
- Watson EB, Brennan JM (1987) Fluids in the lithosphere, 1. Experimentally-determined wetting characteristics of $\text{CO}_2\text{--H}_2\text{O}$ fluids and their implications for fluid transport, host-rock physical properties, and fluid inclusion formation. *Earth Planet Sci Lett* 85:497–515
- Wellman HW, Wilson AT (1965) Salt weathering: neglected geological erosive agent in coastal and arid environments. *Nature* 205:1097–1098
- Wheeler J (2014) Dramatic effects of stress on metamorphic reactions. *Geology* 42:647–650
- Wood BJ, Walther JV (1983) Rates of hydrothermal reactions. *Science* 222:413–415
- Worden RH, Walker FDL, Parsons I, Brown WL (1990) Development of microporosity, diffusion channels and deuteric coarsening in perthitic alkali feldspars. *Contrib Mineral Petrol* 104:507–515
- Yokoyama T, Nakashima S, Murakami T, Mercury L, Kirino Y (2011) Solute concentration in porous rhyolite as evaluated by sequential centrifugation. *Appl Geochem* 26:1524–1534